Interaction of discrete breathers with impurity modes

Kyle Forinash
Indiana University Southeast, New Albany, Indiana 47150

Michel Peyrard
Laboratoire de Physique de l'Ecole Normale Supérieure de Lyon, 46 allée d'Italie, 69007 Lyon, France

Boris Malomed
Department of Applied Mathematics, School of Mathematical Sciences, Tel Aviv University, Ramat Aviv 69978, Israel
(Received 29 November 1993)

We study the interaction between a discrete breather and an impurity in a nonlinear lattice model. Although the existence of the breather is due to nonlinearity while the existence of an impurity mode is due to a mass inhomogeneity, the two modes are very similar and therefore interact strongly. Their interaction provides some insight on the interplay between nonlinearity and disorder which localize energy in a lattice. In particular we show that an impurity can act as a *catalyst* for the fusion of two breathers and the generation of a larger excitation.

PACS number(s): 03.40.Kf, 63.10.+a, 46.10.+z

I. INTRODUCTION

Over the past several years, it has become increasingly apparent that spatially localized nonlinear excitations contribute significantly to the properties of biological molecules. The case of DNA denaturation is an interesting example because, on the one hand, the formation of locally denatured regions is clearly observed in experiments [1], and, on the other hand, very large fluctuations, or breathing, of the double helix are observed [2]. Recent studies have linked these phenomena with the idea that breathers could be precursor to denaturation [3,4]. This poses the question of the mechanism of the growth of these breathers from small thermally excited modes to large denaturation bubbles. The experiments [2] show that the breathers are narrow (i.e., extend over a few lattice sites only) and it has been shown recently that the discreteness of the lattice can provide a mechanism for localization of energy into large breathers [5,6]. However, when one thinks of localization, the possible role of disorder and Anderson localization [7] comes immediately to mind. This could be relevant for DNA since, because it contains the genetic code, the molecule is not homogeneous. The interplay between nonlinearity and disorder is far from being understood [8]. In this work, we want to consider one of its aspects by studying the interaction of discrete breathers with impurities as a possible mechanism leading to energy localization in DNA.

This is not the first time that the interaction of a localized nonlinear excitation in a lattice with an impurity has been studied. In 1979 Yajima studied the scattering of lattice solitons by a mass impurity [9]. More recently, Zhang, Kivshar, and Vázquez showed that in the sine-Gordon [10] or ϕ^4 [11] models, the scattering of a kink by an impurity can exhibit a resonant structure which is associated with an energy exchange between the kink and an impurity mode. Resonances were also found by Malomed *et al.* in the case of a sine-Gordon equation coupled to a linear Klein-Gordon equation with a defect [12]. Although it shows some similarities with these examples, the case of the breather that we consider in this paper is fundamentally different because *the nonlinear excitation that we study and the impurity mode belong to the same type of excitations.* As shown by the work of Sievers and co-workers [13,14] and Kosevich and Kovalev [15], lattice breathers can be viewed as local modes in a lattice where, instead of a mass defect, the localization is intrinsic and due to nonlinearity. Therefore the interplay between a nonlinear localized mode and an impurity mode can be much stronger than between a kink (which has no internal dynamics except perhaps an excited mode as in the ϕ^4 model [16]) and the impurity. For instance, we show that the impurity mode can be used to store energy temporarily from a first breather which is then combined with the energy of a second breather interacting with the impurity mode to form a large single breather. In this case, the impurity really acts as a *catalyst* for the formation of large breathers. This mechanism for energy localization, which, to our knowledge has not been described previously, is discussed in Sec. IV. We present the model, the breather and impurity modes in Sec. II and study the interaction of a single breather with the impurity mode, using numerical simulations and a collective coordinates approach, in Sec. III.

II. BREATHERS AND IMPURITY MODES IN THE LATTICE MODEL

We consider a simple lattice model which was established to represent the dynamics of base pairs in DNA [4], but which is sufficiently general to be applied in other areas of physics. It consists of a chain of harmonically coupled particles subjected to an asymmetric on-site po-

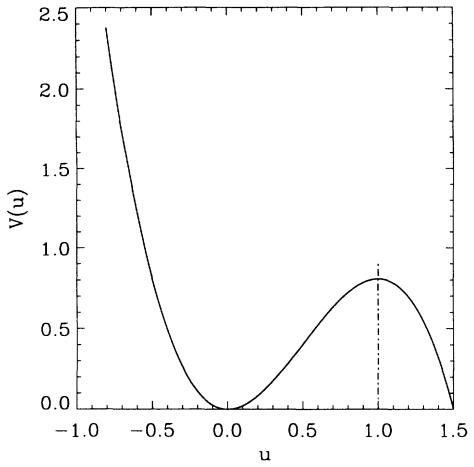

FIG. 1. The on-site potential of the model. We consider only displacements $u < 1$.

tential. In the original application to DNA [17] the potential was a Morse potential, but this can be reduced to a simpler cubic polynomial if we do not consider displacements so large that they would bring the particles onto the plateau of the Morse potential.

The Hamiltonian of the model is

$$H = \sum_n \left[\frac{1}{2}\dot{u}_n^2 + \frac{1}{2}(u_n - u_{n-1})^2 + V(u_n) \right] , \tag{1}$$

where the potential is

$$V(u_n) = \omega_d^2 \left(\frac{u_n^2}{2} - \frac{u_n^3}{3} \right) . \tag{2}$$

It has the shape shown in Fig. 1. In these expressions, the position of particle n is written as a dimensionless variable u_n; time and space have been scaled to have a unit mass for the particles and a harmonic coupling constant equal to unity [4]. The parameter ω_d measures the relative scale of the on-site potential and of the coupling energy. Large values of ω_d correspond to the weakly coupled case where the effects of lattice discreteness are large. In this paper all of the simulations have been performed with $\omega_d = 2.2$. This is a moderately discrete case so that the breathers we investigate are localized on a few lattice sites (which is relevant for DNA [2]), but are not completely trapped by the pinning potential due to the lattice [6].

A. Breathers

The Hamiltonian (1) has large-amplitude breatherlike approximate solutions which are stabilized by discreteness [4]. Solutions which do not move with respect to the lattice can be obtained very accurately with the lattice Green's function method [14,4]. They can have an amplitude approaching 1, i.e., approaching the turning point of the potential, and be perfectly stable. No exact derivation of *moving* breathers is known yet, but approximate solutions can be obtained by looking for envelope solitons in the semidiscrete limit. The method uses an expansion of the displacements $u_n(t)$ as

$$\begin{aligned} u_n(t) = {} & \epsilon \left[F_{1,n}(t) e^{i\theta_n} + \text{c.c.} \right] \\ & + \epsilon^2 \left[F_{0,n}(t) + F_{2,n}(t) e^{i2\theta_n} + \text{c.c.} \right] + O(\epsilon^3) , \end{aligned} \tag{3}$$

with $\theta_n = qn - \omega t$ where q and ω are related by the lattice dispersion relation $\omega^2(q) = \omega_d^2 + 4\sin^2(q/2)$. The functions $F_{i,n}$ are assumed to be slowly varying in time and from site to site, and they are determined in the continuum limit. Following the standard reductive perturbation method, and using the new variables $T = \epsilon^2 t$ and $X = \epsilon(x - V_g t)$ with $V_g = d\omega/dq$, we obtain the nonlinear Schrödinger (NLS) equation for $F_1(X,T)$,

$$iF_{1,T} + PF_{1,XX} + Q|F_1|^2 F_1 = 0 , \tag{4}$$

with

$$Q = \frac{\omega_d^2}{\omega} \frac{5\omega_d^2 + 32\sin^4(q/2)}{3\omega_d^2 + 16\sin^4(q/2)}, \tag{5a}$$

$$P = \frac{\omega_d^2 \cos q - 4\sin^4(q/2)}{2\omega^3}. \tag{5b}$$

The breather solution is given by [4]

$$\begin{aligned} u_n(t) = {} & 2\epsilon A' \operatorname{sech}[\epsilon(n - V_e t)/L_e] \cos(\Theta n - \omega_b t) \\ & + 2\epsilon^2 A'^2 \operatorname{sech}^2[\epsilon(n - V_e t)/L_e] \\ & \times \left\{ 1 - \frac{1}{3 + (16/\omega_d^2)\sin^4(q/2)} \right. \\ & \left. \times \cos[2(\Theta n - \omega_b t)] \right\}, \end{aligned} \tag{6}$$

with

$$\begin{aligned} & A' = \left(\frac{u_e^2 - 2u_e u_c}{2PQ} \right)^{1/2} , \qquad L_e = \frac{2P}{(u_e^2 - 2u_e u_c)^{1/2}}, \\ & V_e = V_g + \epsilon u_e , \qquad \Theta = q + \epsilon u_e / 2P, \\ & \omega_b = \omega + (V_g + \epsilon u_c)\epsilon u_e / 2P. \end{aligned}$$

The parameters u_e and u_c, which are the velocities of the envelope and carrier waves, determine the characteristics of the solution together with the wave vector q chosen for the carrier wave. In our simulations we have chosen $q = 0.2$, and the envelope velocity u_e and amplitude A' as input parameters. Other parameter values are determined from these chosen values.

Figure 2 shows one example of such a breather propagating in the homogeneous lattice. Its initial input parameters $A' = 0.28$ and $u_e = -0.20$ give rise to a breather with an initial amplitude of $A_0 = 0.66$ and velocity $V_e = -0.11$. This initial condition is not an exact solution for the lattice and after a time delay $t = 50$, its measured amplitude is $A = 0.62$ and its velocity from the simulation is $v = -0.16$. In the following, we shall characterize the breathers by their input amplitude A_0 and

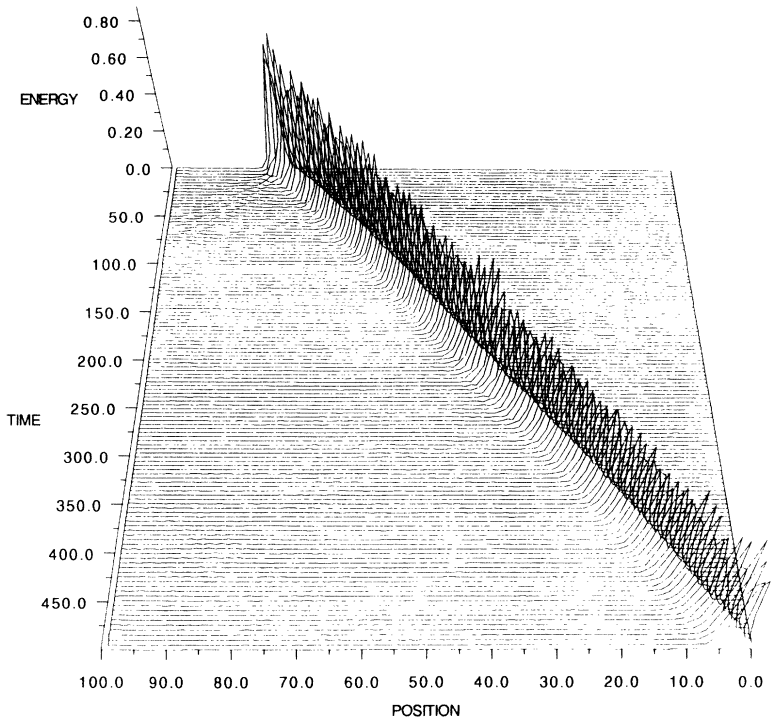

FIG. 2. Propagation of a breather in a homogeneous lattice. Breather input parameters are $\omega_d = 2.2$, $u_e = -0.2$, and $A' = 0.28$.

velocity V_e although the results are for breathers interacting after a time delay of approximately $t = 50$ because A_0 and V_e are well defined quantities while the exact amplitude and velocity of a breather when it interacts with the impurity may depend on the details of the collision.

B. Impurity modes

When the lattice contains a mass impurity at site 0, i.e., when the masses of the particles are equal to $m_n = 1 + \Delta m\, \delta_{n,0}$, it can have a local mode, even in the linear limit. In this limit, the discrete set of equations of motion which derive from Hamiltonian (1) reduces to

$$m_n \ddot{u}_n - (u_{n+1} + u_{n-1} - 2u_n) + \omega_d^2 u_n = 0\,, \qquad (7)$$

and, for an isolated impurity these equations can be solved exactly. For $n > 0$ or $n < 0$, they have solutions of the form

$$u_n(t) = e^{i\omega_i t}\, r^n, \qquad (8)$$

where r is a solution of

$$r^2 - (2 + \omega_d^2 - \omega_i^2) r + 1 = 0\,. \qquad (9)$$

This equation has two roots r_1 and r_2, such that $r_1 r_2 = 1$. Denoting by r_1 the root which has a modulus smaller than 1, we get localized solutions if we chose $r = r_1$ for $n > 0$ and $r = r_2$ for $n < 0$ in Eq. (8). Then, solving Eq. (7) at site $n = 0$ with u_1 and u_{-1} given by Eq. (8) determines the possible values of the frequency ω_i of the impurity mode. We are interested in modes which are in the range $0 < \omega_i < \omega_d$, which is also the frequency range for breathers. They are found for $\Delta m > 0$. Their frequency is given by

$$\omega_i^2 = [(\omega_d^2 + 2) - \sqrt{4 + \Delta m^2(\omega_d^4 + 4\omega_d^2)}]/(1 - \Delta m^2) \qquad (10)$$

and their shape is determined by Eq. (8) with

$$r = r_1 = \{(2 + \omega_d^2 - \omega_i^2) - [(\omega_d^2 - \omega_i^2)(\omega_d^2 - \omega_i^2 + 4)]^{1/2}\}/2. \qquad (11)$$

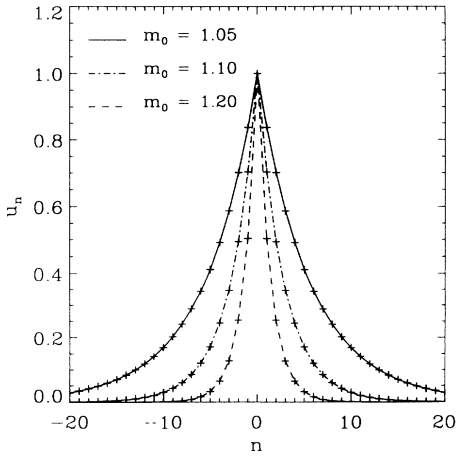

FIG. 3. Aspect of the linear impurity mode for various values of m_0. Note that when m_0 is very close to 1, the mode extends over many lattice sites, while for larger values of m_0 its width becomes comparable to the width of the breathers that we are considering (see Fig. 2).

TABLE I. Theoretical frequencies (in second row) compared to simulation frequencies (all other rows) of small-amplitude impurity modes. †Amplitudes of this magnitude for this impurity mode are unstable in the simulation.

$m+\Delta m$	1.025	1.05	1.1	1.2	1.4
Theoretical frequency	0.34995	0.34961	0.34809	0.34266	0.32703
Amplitude	Observed frequencies				
0.1	0.349	0.348	0.348	0.343	0.328
0.2	0.346	0.348	0.348	0.342	0.326
0.3	0.338	0.334	0.343	0.338	0.323
0.4	†	0.323	0.333	0.333	0.318
0.5	†	†	0.322	0.323	0.313
0.6	†	†	†	0.313	0.303

For small mass defects, ω_i approaches the bottom of the lattice phonon band ω_d and r_1 tends to 1, i.e., the mode has a very large spatial extension. It gets more and more localized as Δm increases. Figure 3 shows the shape of the linear impurity mode for various values of m_0.

We are interested here in excitations of this mode by large-amplitude breathers and consequently its amplitude may go beyond the linear approximation. We have therefore studied the stability of the impurity mode by numerical simulations using a fifth order Runge-Kutta method [18] on a chain of 100 atoms. Profiles of the theoretical impurity modes were used as initial conditions. As expected, at small amplitudes, when the linear approximation is valid, the impurity mode has been found to be very stable and its frequency is in very good agreement with Eq. (10). At large amplitude, the initial condition generates a stable impurity mode only if Δm is sufficiently large. Similar to the results found for discrete breathers [4] we notice that narrower excitations are more stable. The frequency of the nonlinear impurity mode for large amplitudes drops significantly below the linear frequency, as shown in Table I.

III. COLLISIONS OF BREATHERS WITH AN UNEXCITED IMPURITY

A. Numerical results

We have investigated the properties of a breather in the presence of a mass impurity with numerical simulations of the equations of motion resulting from the Hamiltonian (1). The equations of motion of a chain with 100 particles with periodic boundary conditions were integrated with a fifth order Runge-Kutta method [18]. Energies were calculated directly from the model and were conserved in all cases to better than 0.001%. We consider first the simplest case of an impurity which is initially at rest. Even in this case, the simulations show a rich behavior depending on the amplitude and velocity of the breather. Figure 4 shows four typical behaviors of a breather colliding with an impurity at rest. It can either pass through (a), be trapped by the impurity (b), split into a trapped impurity mode and a smaller reflected breather (c), or be almost totally reflected (d) leaving only a small excitation at the impurity site. A summary of the results of colliding several different breathers with various mass impurities is shown in Table II. The breather amplitude A_0 is given in the first column along with its frequency (in parentheses) as measured from the simulation using the maximum entropy method [18].

For very light impurities ($m \leq 1.05$), the frequency of the impurity mode is always higher than the breather frequency. The breather has no difficulty in setting the light mass in motion, but, as its frequency is not resonating with that of the impurity mode, it passes through the impurity, leaving it almost unexcited. A similar case of "reversible" excitation of an impurity mode by a nonlinear excitation has been studied for a sine-Gordon equation coupled to a linear Klein-Gordon equation with a defect [12]. Heavy impurities ($m \geq 1.4$) have frequencies which are below the breather frequencies. They behave almost as "fixed" obstacles that reflect the breather. An examination of Fig. 4 shows that, in fact, the impurity mode is temporarily excited but its energy is almost immediately restored to the reflected breather.

In the intermediate cases, the breather frequency is close to the frequency of the impurity mode and a strong interaction can occur. Cases listed as T in Table II are cases of nearly complete trapping with only small amounts of energy escaping. The case labeled "SPLIT" is a 50-50 split in the energy of the breather between passing and reflecting. The resulting pulses in that case are no longer of sufficient amplitude to maintain a breather profile and therefore disperse. Cases labeled R in the table are cases of 100% reflection. In other cases a portion of the energy is reflected and a portion trapped. In these cases of partial reflection, the percentage of energy reflected (given by %R) was determined by comparing

TABLE II. Cases of passing (P), trapping (T), and reflection (R) of breathers by several mass defects. Input amplitudes A_0 of the breather are given in the first column. The values in parentheses are frequencies measured from the simulations before (left column) and after the scattering (all other columns).

$m+\Delta m$	1.025 defect	1.05 defect	1.1 defect	1.2 defect	1.4 defect
Breather					
0.55(0.343)	P(0.343)	P(0.343)	SPLIT	R(0.348)	R(0.341)
0.61(0.342)	P(0.339)	P(0.341)	T(0.343)	91%R(0.342)	R(0.338)
0.66(0.335)	P(0.336)	P(0.341)	T(0.339)	80%R(0.340)	R(0.342)
0.72(0.329)	P(0.332)	T(0.335)	T(0.329)	40%R(0.349)	96%R(0.331)
0.77(0.323)	P(0.328)	T(0.328)	T(0.327)	32%R(0.345)	91%R(0.332)

the energy of three atoms centered on the maximum energy atom of the reflected pulse with the energy of the three atoms centered on the impurity. The frequencies (in parentheses) were measured after collision. In the cases with partial trapping and reflection the frequencies are those of the reflected pulse.

The analysis of the phenomena requires more than simply matching frequencies, however. One important aspect is also the spatial extent of the impurity mode. The breather extends over a few lattice spacings and this is comparable to the spatial extent of the impurity mode for intermediate values of m as shown in Fig. 3. For $m = 1.1$, the breather matches not only the frequency of the impurity mode, but also its shape. This can explain why, when the breather reaches the impurity site, it stays trapped. For larger impurities (for instance, $m = 1.2$), the lower-amplitude breathers have frequencies that do not overlap with the frequency of an impurity mode of the same am-

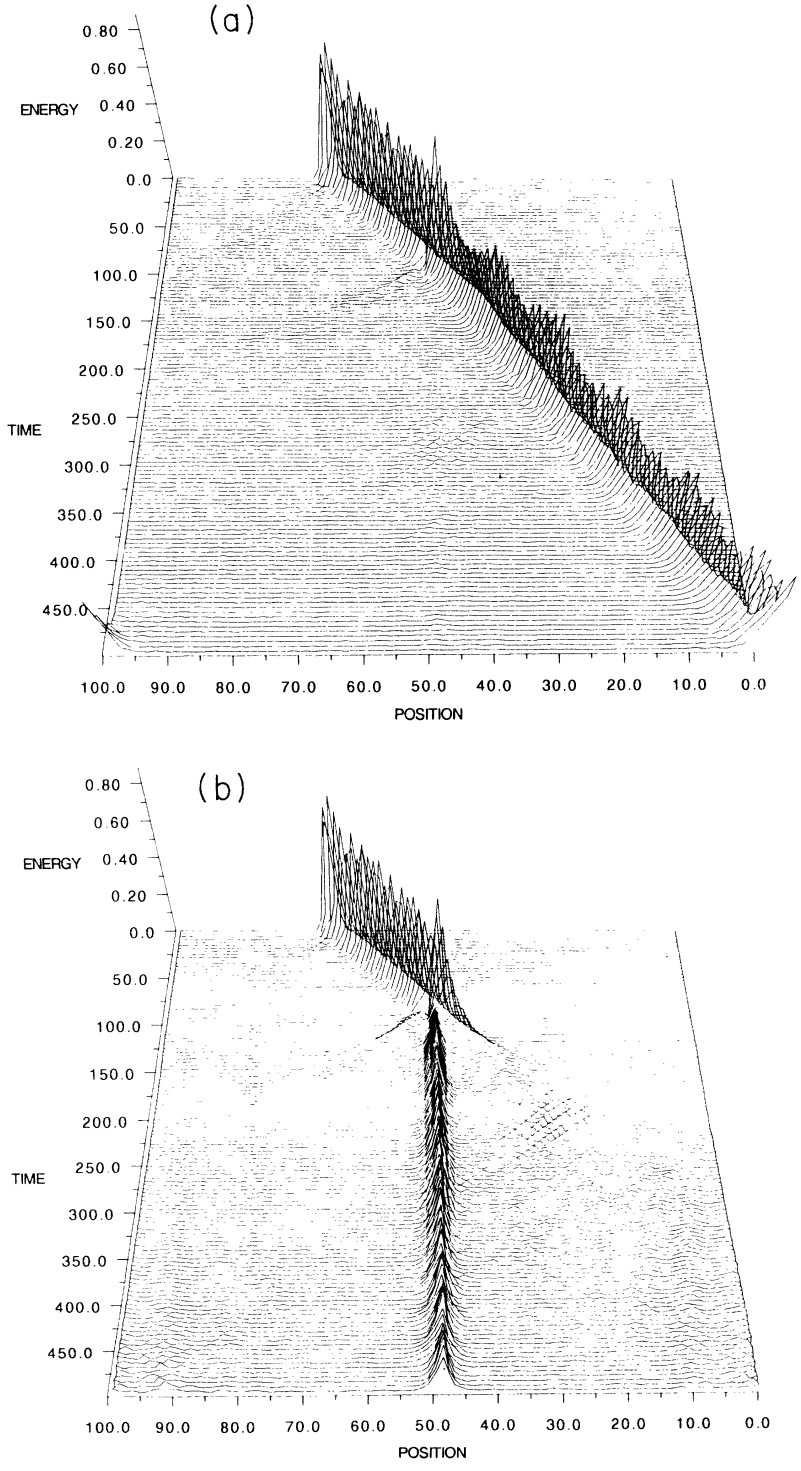

FIG. 4. Typical results of the collision of a breather with an unexcited impurity: Passing (a), trapping (b), partial reflection (c), and reflection (d) of a breather by unexcited mass defects of 1.025, 1.1, 1.2, and 1.4, respectively, located at site 50. Breather input parameters are $\omega_d = 2.2$, $u_e = -0.2$, and $A' = 0.28$.

plitude and consequently they are not trapped. When the amplitude of the breather increases, causing also an increase of the amplitude of the local mode which is excited during the collision, the variation of the frequencies with amplitude for both the breather and the local mode are such that the resonance condition is approached. As a result, a larger and larger fraction of the energy of the incoming breather stays trapped at the impurity site, as shown in Table II.

B. Collective coordinate analysis

The discussion of the results of the numerical simulations shows that their interpretation is complex because it involves the variation of the frequencies with amplitude and the spatial extent of the excitations. In order to get a better understanding of these results, it is interesting to develop a collective coordinate approach to investigate the evolution of the breather and impurity mode. The

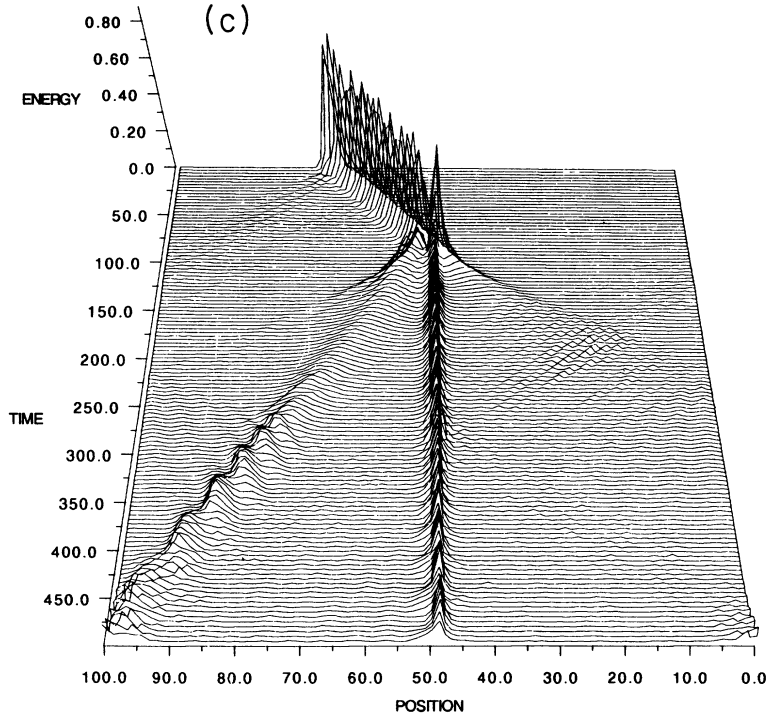

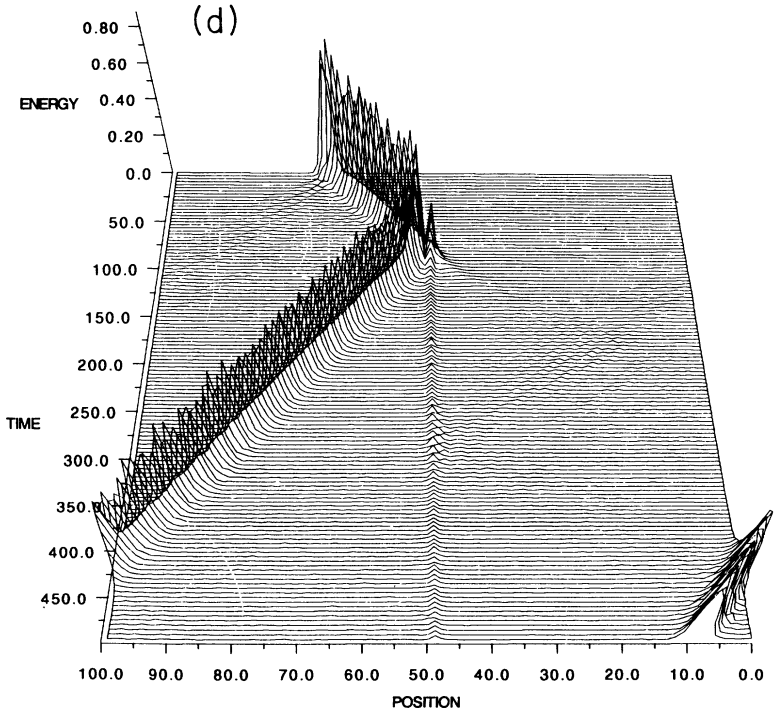

FIG. 4. (*Continued*).

validity of such an approach is limited by the lack of a good analytical description of the breathers in a discrete lattice. However, useful results can be obtained if one starts from the approximate nonlinear Schrödinger equation (4) obtained in the semidiscrete limit. This equation has to be extended to include the mass defect. This is easily achieved if one considers that the mass defect Δm is of the order ϵ^2 by writing $m_n = 1+\epsilon^2\Delta m\,\delta(n)$. In this case, carrying out the reductive perturbation method as before, when one writes the cancellation of secular terms at order ϵ^2 which leads to the NLS equation for F_1, one finds an extra term $\Delta m\,\delta(n)\,(\partial^2/\partial t^2)[F_{1,n}\exp(i\theta_n)]$. After making the continuum limit approximation for $F_{1,n}$, and changing again to the frame moving at the group velocity of the carrier wave V_g by defining $T=\epsilon^2 t$ and $X=\epsilon(x-V_g t)$, we get the perturbed NLS equation

$$iF_{1,T}+PF_{1,XX}+Q|F_1|^2F_1 +\frac{1}{2}\Delta m\,\omega\,\delta(X+V_gT)\,F_1=0\,, \quad (12)$$

where P and Q have the same values as before. As we are looking for breathers with a frequency close to ω_d, we can restrict ourselves to carriers with $q\approx 0$, i.e., $\omega\approx\omega_d$, and $P=1/2\omega_d$, $Q=5\omega_d/3$, $V_g=0$. In order to simplify the notation for the collective coordinate calculations, it is also convenient to rescale F_1 into $G=\sqrt{5/3}\,F_1$ and to define new time and space variables by $\tau=\omega_d t$, $\xi=\omega_d X$, so that the perturbed NLS equation takes the standard form

$$iG_\tau+\frac{1}{2}G_{\xi\xi}+|G|^2G+\gamma\,\delta(\xi)\,G=0\,, \quad (13)$$

where $\gamma=\Delta m/2$.

In the absence of impurity ($\gamma=0$), this equation has the soliton solution

$$G=\eta\,\mathrm{sech}\,\eta(\xi-v\tau)\,e^{i(v\xi+\alpha\tau)}\,, \quad (14)$$

with $\alpha=(\eta^2-v^2)/2$, which was used to write the solution (6). In the linear limit, $\gamma>0$, it has a solution localized around $\xi=0$ given by

$$G=a\sqrt{\lambda}\,e^{-\lambda|\xi|}\,e^{i\Omega t}\,, \quad (15)$$

with $\lambda=\gamma$, $\Omega=\lambda^2/2$. Written in the original coordinates where $u\propto G\exp(-i\omega_d t)$, this mode corresponds to the continuum limit of the impurity mode given by Eq. (8). Its frequency is $\omega_i'=\omega_d(1-\Delta m^2/8)$.

In order to provide an approximate description of the interaction of a breather with the impurity mode, we use an ansatz for the field configuration which is a combination of the soliton and impurity mode,

$$G(\xi,\tau)=\eta\,\mathrm{sech}(\eta\xi-z)\,e^{i(\phi+k\xi)}+a\sqrt{\lambda}e^{-\lambda|\xi|+i\phi+i\psi}\,, \quad (16)$$

where the parameters η, z, ϕ, k, a, λ, and ψ are arbitrary functions of τ. This ansatz, introduced in the Lagrangian for the field equation, (13), gives

$$L=\int_{-\infty}^{+\infty}\Lambda d\xi\,, \quad (17)$$

with

$$\Lambda=\frac{1}{2}i(G^*G_\tau-GG_\tau^*)-\frac{1}{2}|G_\xi|^2+\frac{1}{2}|G|^4+\gamma|G|^2\delta(\xi)\,. \quad (18)$$

In the calculation we neglect all the terms produced by overlapping of the two parts of the ansatz, *save* those produced by the term proportional to γ in Λ. Physically this means that we ignore the direct interaction between the soliton and the local mode, except for the energy exchange occurring *through the defect*. Besides the practical reason that it makes the calculation possible there are several justifications to this simplification. First, we know that solitons and linear modes are independent excitations except in the presence of perturbations, so it is reasonable to assume that the defect-mediated interaction is dominant. Second, if one includes the extra interaction terms in the calculation one notices that, contrary to the terms that we keep, they contain rapidly varying phase factors so that their integral over space would be very small. With this assumption, the calculation is simple and yields

$$L=-2\eta\dot\phi-2\dot k z-a^2(\dot\phi+\dot\psi)+\frac{1}{3}\eta^3-k^2\eta-\frac{1}{2}a^2\lambda^2 +\gamma\eta^2\mathrm{sech}^2 z+2\gamma\eta a\sqrt{\lambda}\,\mathrm{sech}z\cos\psi+\gamma a^2\lambda+O(a^4)\,. \quad (19)$$

The variational equations corresponding to Lagrangian (19) determine the time evolution of the various parameters in the ansatz.

First of all, the variation in ϕ gives

$$\frac{d}{d\tau}\left[\eta+\frac{1}{2}a^2\right]=0, \quad (20)$$

which has simply the meaning of the conservation of the wave action

$$\int_{-\infty}^{+\infty}|G|^2d\xi=C\,. \quad (21)$$

The other equations are

$$\dot z=\eta k, \quad (22a)$$

$$\dot k=-\gamma\eta^2\mathrm{sech}^2 z\tanh z-\gamma\eta a\sqrt{\lambda}\cos\psi\,\mathrm{sech}z\tanh z, \quad (22b)$$

$$\dot\psi=-\frac{1}{2}\eta^2+\frac{1}{2}k^2-\gamma\eta\,\mathrm{sech}^2 z-\gamma a\sqrt{\lambda}\cos\psi\,\mathrm{sech}z -\frac{1}{2}\lambda^2+\gamma\eta a^{-1}\sqrt{\lambda}\cos\psi\,\mathrm{sech}z+\gamma\lambda, \quad (22c)$$

$$\dot a=\gamma\eta\sqrt{\lambda}\sin\psi\,\mathrm{sech}z, \quad (22d)$$

$$a(\gamma-\lambda)+\gamma\eta\lambda^{-1/2}\cos\psi\,\mathrm{sech}z=0\,. \quad (22e)$$

The variation with respect to η gives also an equation for $\dot\phi$ which is not displayed because ϕ does not appear in the equations which are important to us, i.e., which determine the evolution of the position z and amplitude η

of the breather, and of the amplitude $a\sqrt{\lambda}$ of the localized mode. Equation (22d) plays a crucial role because it demonstrates that the moving soliton excites the local mode. Note that, in the absence of the soliton ($\eta = 0$), the algebraic equation (22e) gives the correct value $\lambda = \gamma$ for the spatial decay of the impurity mode.

The system of Eqs. (20) and (22) is too complicated to be solved analytically. It has one integral of motion which is given by the Hamiltonian derived from the Lagrangian (19). Using Eq. (22e) it can be written as

$$H' = \eta k^2 - \frac{1}{3}\eta^3 - \gamma\eta^2 \mathrm{sech}^2 z + \gamma a^2\lambda - \frac{3}{2}a^2\lambda^2 . \quad (23)$$

In order to analyze the results of the numerical simulations of the full system described in the preceding section, we have followed numerically the evolution of the collective coordinates determined by Eqs. (20) and (22). This system of equations can be integrated with initial conditions corresponding to the simulations performed on the full system, i.e., a local mode initially at rest and a breather situated far from the position $z = 0$ of the impurity (for instance, $z = -10$). Far from the defect the breather velocity is given by k, so that the initial value k_0 corresponds to the initial velocity V_e used in the simulations. The other parameters are initially set to 0. At each step of the integration, z, k, ψ, and a are evolved according to Eqs. (22a)–(22d). Then the soliton amplitude is determined with the conservation relation (20) and the algebraic equation (22e) is used to calculate λ. Care must be taken when solving this equation because it is a cubic equation in $\sqrt{\lambda}$, which does not have a unique solution when the soliton interacts strongly with the impurity. The appropriate solution is selected by continuity and through the conservation of the Hamiltonian (23).

One cannot expect the collective coordinate analysis to give a quantitative account of the full simulations because we know that the NLS equation (13) which is used as the basis of this analysis gives only an approximate description of the dynamics of the discrete lattice. However, the collective coordinates give a good qualitative description of the dynamics of the full system and they provide additional information because they allow us to follow independently the evolution of the breather and of the local mode. Figure 5 is the counterpart of Fig. 4. It shows the position and amplitude of the breather, and the amplitude of the local mode for collisions with different impurities. For the lightest impurity ($\gamma = 0.02$, i.e., $m = 1.04$), the breather passes through the impurity almost unaffected. The impurity mode, which is excited during the collision, comes back to a very small level of excitation after the breather has passed. For the heaviest impurity ($\gamma = 0.14$, i.e., $m = 1.28$), the breather is almost totally reflected and leaves an impurity mode which is again almost unexcited. At the collision time, however, Fig. 5(b) shows that the impurity mode is strongly excited while the breather amplitude decreases drastically. This phenomenon is clearly visible in Fig. 4(d) corresponding to full simulations, showing that the collective coordinates give a good account of the details of the interaction. The case of intermediate γ is more complicated. One generally finds a trapping of the breather at the impurity site as shown in Fig. 5(c). In this case the collective coordinates provide information that the full simulations cannot give because they show that, although it oscillates, the breather amplitude stays

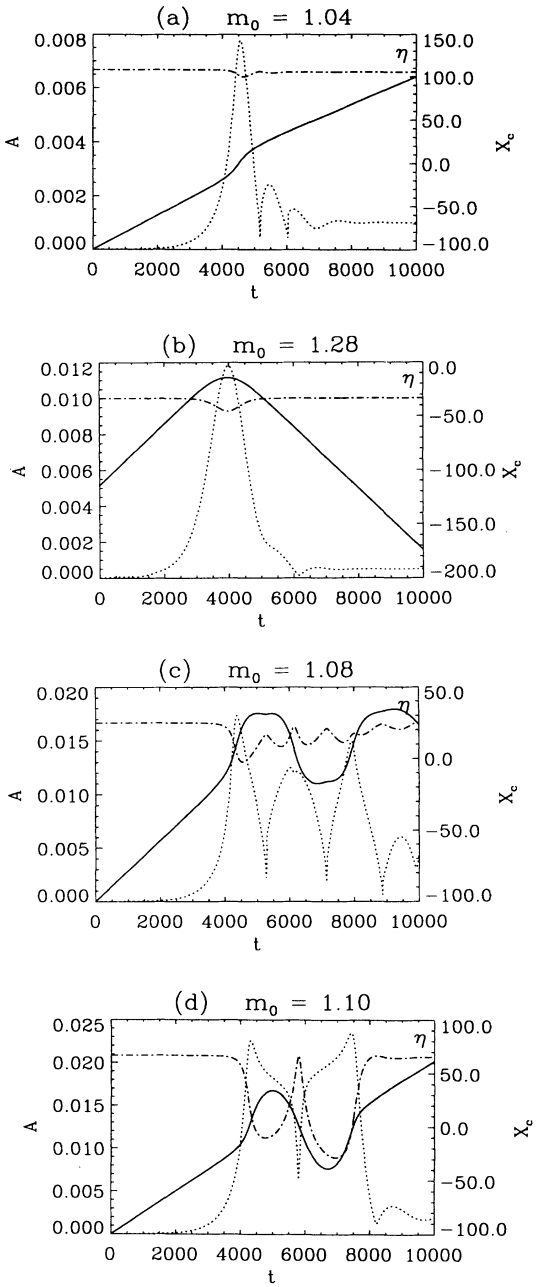

FIG. 5. Results of the integration of the collective coordinate equations for typical cases of a breather interacting with an unexcited impurity: Position of the breather (solid line, scale X_c on the right axis) and amplitude of the local mode (dotted line, scale $a\sqrt{\lambda}$ on the left axis) versus time. The dash-dotted line labeled η shows the breather amplitude versus time. Its scale is not explicitly indicated but the evolution of η versus time can be appreciated with respect to the initial value $\eta = 0.10$. (a) $m_0 = 1.04$ ($\gamma = 0.02$); the breather passes through the defect. (b) $m_0 = 1.28$ ($\gamma = 0.14$); the breather is reflected. (c) $m_0 = 1.08$ ($\gamma = 0.04$); the breather is trapped at the impurity site. (d) $m_0 = 1.10$ ($\gamma = 0.05$); example of a resonance window.

large while the amplitude of the impurity mode, $a\sqrt{\lambda}$, remains low. Therefore one can really speak of a trapped breather rather than a large impurity mode excited by the breather.

The collective coordinates also show additional behaviors such as the one plotted in Fig. 5(d). In the range of γ that gives trapping, the collective coordinate calculation finds narrow windows of *resonances* in which the breather passes beyond the impurity, oscillates a few times around the impurity site, and is finally reflected or transmitted. These results are very similar to the resonant structures observed in the sine-Gordon [10] or ϕ^4 [11] models and have the same interpretation. But the simulations on the full system show that these narrow resonances are very vulnerable to perturbations, like the lattice discreteness. In spite of careful search, we have found only one case which can be interpreted as such a window, as shown in Fig. 6. In this case the breather is trapped for a very long time at the impurity site and escapes at low velocity. Its oscillation around the impurity site is, however, not clearly detected. General observations, valid also in the case of reflection, show that in the simulations on the full system the breather is more confined around the impurity site during the collisions than is found in the collective coordinate approach. From the results of the collective coordinate calculations regarding the values of γ that produce transmission, reflection, or trapping, one concludes that this method leads to results which are in very good agreement with the results of the simulations listed in Table II. This is, however, only true because the collective coordinate calculations have been conducted with very small breather initial velocity ($k_0 = 0.02$) compared to the velocity used in the simulations of the full system ($V_e = 0.11$). This means that the interaction between the breather and the impurity mode, given by a continuum limit calculation, is much weaker than the real interaction in a discrete lattice. A similar observation was made previously for the scattering of a kink by a mass impurity in the sine-Gordon model: a continuum limit calculation never finds a kink reflection while a discrete calculation does [19]. The collective coordinate calculations give a good idea of the mechanism of the energy exchange between the breather and the defect, but the intensity of this exchange is not correctly predicted.

TABLE III. Dependence of the collision output on distance of the breather launch site from the excited impurity. Breather parameters are $\omega_d = 2.2$, $V_e = -0.11$, and $A_0 = 0.66$. The impurity of mass 1.05 was given an initial impurity mode profile (given in the text) with initial amplitude of 0.2.

Launch distance from defect	11	12	13	14	...	26	27	28	29
Result	T	P	T	P	...	T	P	T	P

IV. COLLISION OF A BREATHER WITH AN EXCITED IMPURITY

If one now considers the collision of a breather with an excited impurity, the results are much more complex because they depend on the relative phase of the breather and the impurity mode. This is shown in Table III, which gives the output of such a collision as a function of the initial position of the breather. Defects near the threshold between passing and trapping were tested in these simulations. From the table one notices an alternating sequence of pass and trap situations. As the distance between the breather and impurity is changed slightly, the phase of the breather is different when it arrives at the impurity. The results of Table III suggest that the outcome of the collision is highly sensitive to this phase. This can be demonstrated by the collective coordinate calculations because the variable ψ that we introduced is the relative phase of the breather and impurity mode. Changing its initial value in a case which is close to the threshold between trapping and passing through, we can check that the output of the collision is completely modified. This is illustrated in Fig. 7. The results were obtained with the collective coordinates calculations and only the initial phase difference between the breather and impurity mode has been modified in the four cases shown. For $\psi_0 = -\pi/2$, the breather passes through the impurity and takes away a large part of the energy of the impurity mode. As a result its amplitude and velocity increase while the amplitude of the impurity mode is divided by 4 after the collision [Fig. 7(a)]. For $\psi_0 = 0$ the breather is still able to pass through the impurity but its energy gain is small and the impurity mode is also weakly modified

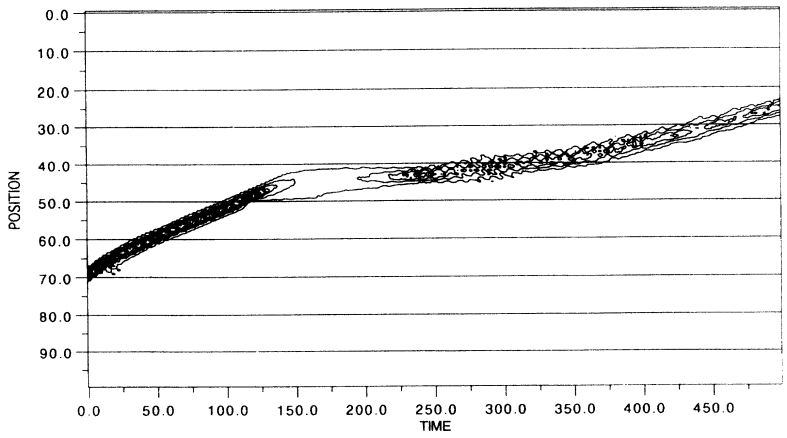

FIG. 6. Example of a breather-impurity collision which almost gives rise to a resonance. We show the energy density in the lattice versus time in a contour plot. The breather is trapped a very long time at the impurity site before escaping at low velocity. The mass of the defect was 1.068 with breather input parameters of $\omega_d = 2.2$, $u_e = -0.3$, and $A' = 0.3$.

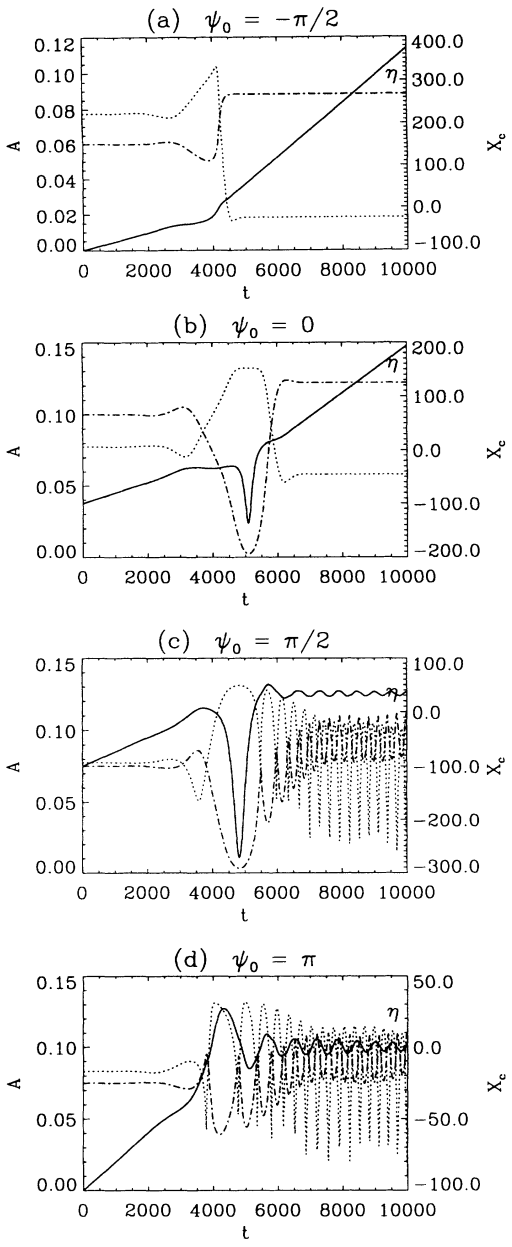

FIG. 7. Role of the phase difference between the breather and impurity mode in a collision as shown by a collective coordinate calculation. The initial values of the collective coordinates are chosen to be near the threshold of trapping: $\gamma = 0.06$, $k_0 = 0.02$, $a_0 = 0.3164$ (which gives an initial amplitude of 0.0775 for the impurity mode which is close to the one used in the simulations of the full system), $\eta_0 = 0.150$ [which, according to Eq. (20), gives an initial value of $\eta = 0.1$ for the breather amplitude parameter]. The initial phase difference between the breather and impurity mode is $\psi_0 = -\pi/2$ in (a), $\psi_0 = 0$ in (b), $\psi_0 = +\pi/2$ in (c), and $\psi_0 = +\pi$ in (d). As in Fig. 5, the solid line indicates the position of the breather center and corresponds to the scale X_c on the right axis. The dotted line indicates the amplitude $a\sqrt{\lambda}$ of the local mode and corresponds to the scale of the left axis. The dash-dotted line labeled η shows the breather amplitude versus time. Its scale is not explicitly indicated but the evolution of η versus time can be compared to the initial value of $\eta = 0.10$. Note the qualitative change between the output of the collision according to the value of ψ_0.

after the collision. For $\psi_0 = \pi/2$ or $\psi_0 = \pi$ the breather stays trapped at the impurity site.

It may seem of little interest to list results so sensitive to the initial conditions, but the interaction of a breather with an excited impurity can have a much more important consequence if one thinks that the impurity can be excited by a *first* breather. Then its effect on a *second* breather that follows the first can vary extensively according to the distance between the two breathers. Figure 8 gives an idea of this possibility on a chain of 100 particles with an impurity of mass $m = 1.082$ at site 50. A first breather of input amplitude $A_0 = 0.66$ is started from site 60 and, if it is alone, is trapped by the impurity [Fig. 8(a)]. If it is followed closely by a second identical breather starting from sites 65–80, the final state depends strongly on the initial distance between the two breathers. We show a few representative cases which are interesting. If the second breather is launched from site 65 [Fig. 8(b)], the first one passes through the impurity losing some amplitude and the second is trapped. A more interesting behavior is found when the second breather is launched from site 68 [Fig. 8(c)]. The first breather is trapped and the second one is also captured by the excited impurity, giving rise to a large, combined breather, formed beyond the impurity (at site 40). This big breather is then attracted by the impurity and finally captured by the impurity site. In other cases, with different initial conditions (second breather at site 70, for instance), the large breather is mobile. The interest of this example is that it shows how the impurity can act *as a perturbation able to induce the fusion of two breathers.* In this case the disorder, which corresponds to the presence of impurities, can provide a mechanism for nonlinear energy localization.

V. CONCLUSION

In this analysis of the interaction of breathers with impurities we have shown that mass defects are very efficient in modifying the dynamics of breathers in a lattice. A local change of only 5% to 10% of the particule mass is sufficient to trap a breather. One reason for such a sensitivity is that the impurity mode and the breather are two dynamical entities which are very similar, and in particular have frequency domains which can overlap. Another reason is the role of discreteness. The collective coordinate calculations, which do not explicitly include discreteness, predict the type of breather-impurity interaction that we have found, but with a much smaller amount of energy exchanged than in the lattice case. This is why trapping or reflection of breathers is found in the collective coordinate case only at very low breather velocities. In the lattice the situation is different because the breather does not propagate freely. It is affected by a strong pinning potential due to the lattice and therefore is more easily trapped. Even with the moving breather that we have considered here, the discreteness effect exists and shows up as oscillations of the amplitude and velocity of the breather as it moves along the lattice. Moreover, the discrete nature of the breather and impurity mode which, in

the case studied extend over only a few lattice sites, appears to cause a stronger interaction than in the continuum case. We are not able to calculate this analytically yet because we lack a good equation to describe moving discrete breathers. In particular we have verified that the discrete Ablowitz-Ladik equation, proposed recently as a possible model to study discreteness effects on breathers [20], gives poor quantitative estimations, particularly for a cubic on-site potential [21], although it does give good qualitative predictions.

The similarity between the breather and impurity mode, which may explain their strong interplay, is very important when one considers the interaction of a breather with an excited impurity, or when one sends successive breathers toward an impurity at rest. The ability of the impurity mode to store energy which can be restored to incoming breathers is responsible for a very rich behavior. From these results one could imagine using the impurity for "signal processing" of the breathers because the system is able to detect in a very sensitive way the distance between successive energy pulses and produce different outcomes according to this distance. The

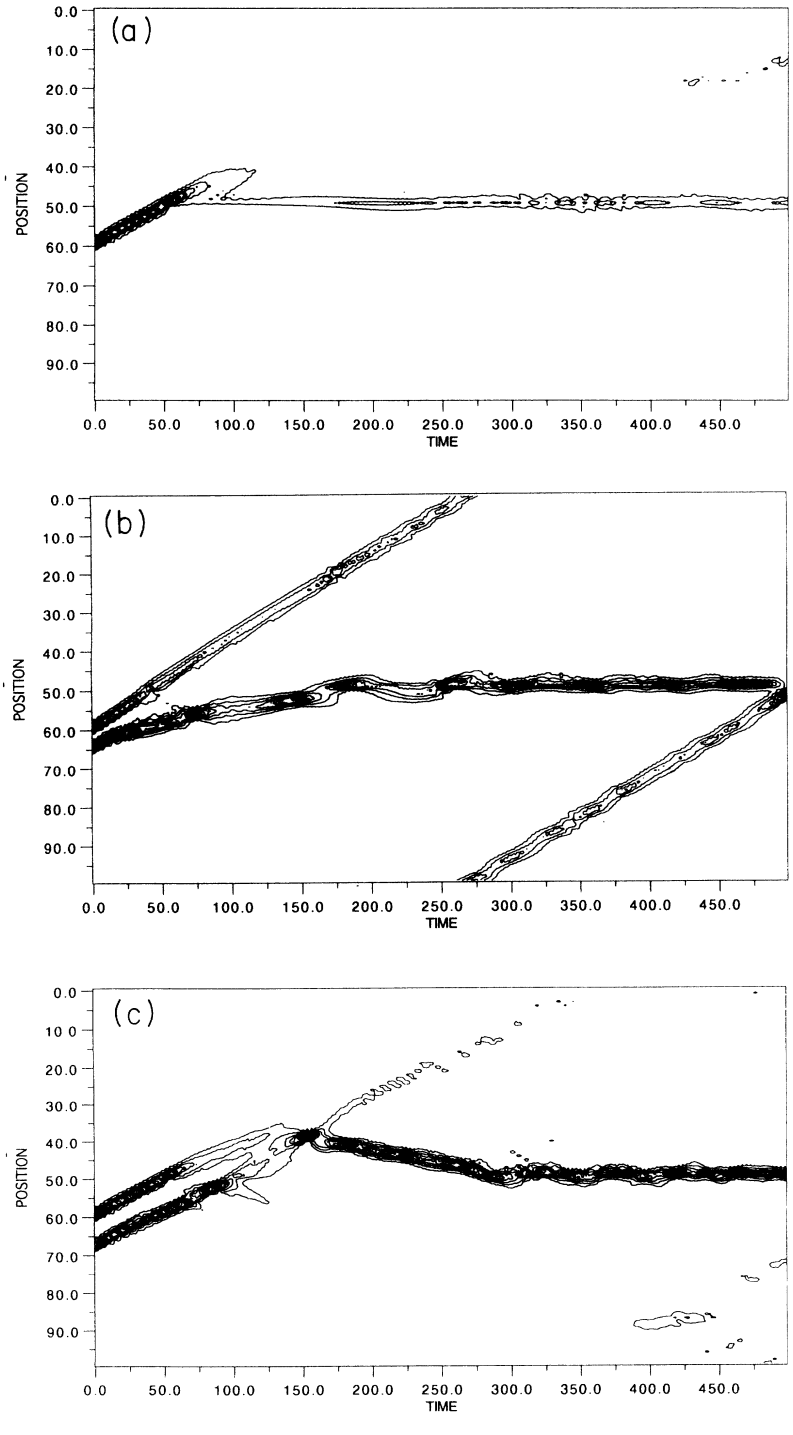

FIG. 8. Collision of two breathers following each other with an unexcited impurity for various values of the distance between the incoming breathers. The defect has a mass $m = 1.082$ and is situated at site 50. A first breather of amplitude $A' = 0.28$ and $u_e = -0.2$ is started at site 60. A second identical breather is launched behind the first with various starting positions: (a) first breather alone; it is trapped by the impurity; (b) with a second breather starting at site 65; (c) with a second breather starting at site 68.

summing of dendrite inputs causing an action potential to form on a nerve fiber comes to mind here, since this is a case of adding several smaller impulses to form a larger above threshold signal, a process which also depends somewhat on the timing of the input signals. The consequence which is probably much more important for physics is that our results show that *the disorder associated with impurities can act as a catalyst* for nonlinear energy localization because it can cause the fusion of two nonlinear excitations into a single larger one. Therefore these results show that disorder and nonlinearity should not be viewed as two *separate* effects that can lead to energy localization. Rather, they can *cooperate* for this localization. This is perhaps the case for the formation of the denaturation bubble in DNA and would explain why some sequences are active sites for the initiation of the denaturation or transcription. This may also be of more general applicability in physics.

ACKNOWLEDGMENTS

We would like to thank T. Dauxois and O. Bang for helpful discussions. K.F. acknowledges the hospitality of the Laboratoire de Physique de l'Ecole Normale Supérieure de Lyon where part of this work was done. K.F. also acknowledges the cooperation of Computer Services at I.U.S. for assistance in computing. Part of this work has been supported by the CEC grant SC1-CT91-0705. The Laboratoire de Physique de l'Ecole Normale Supérieure de Lyon is "Unité recherche associée au CNRS No. 1325."

[1] W. Saenger, *Principles of Nucleic Acid Structure* (Springer-Verlag, Berlin, 1984).
[2] M. Gueron, M. Kochoyan, and J.-L. Leroy, Nature (London) **328**, 89 (1987).
[3] T. Dauxois, M. Peyrard, and A. R. Bishop, Phys. Rev. E **47**, 684 (1993).
[4] T. Dauxois, M. Peyrard, and C. R. Willis, Physica D **57**, 267 (1992).
[5] T. Dauxois and M. Peyrard, Phys. Rev. Lett. **70**, 3935 (1993).
[6] T. Dauxois, M. Peyrard, and C. R. Willis, Phys. Rev. E **48**, 4768 (1993).
[7] P. W. Anderson, Phys. Rev. **109**, 1492 (1958).
[8] *Nonlinearity With Disorder,* Proceedings of the Tashkent Conference, Tashkent, Uzbekistan, October 1990, edited by F. Abdullaev, A. R. Bishop, and S. Pnevmatikos (Springer-Verlag, Berlin, 1992).
[9] N. Yajima, Phys. Scr. **20**, 431 (1979).
[10] Zhang Fei, Yu. S. Kivshar, and L. Vázquez, Phys. Rev. A **45**, 6019 (1992).
[11] Zhang Fei, Yu. S. Kivshar, and L. Vázquez, Phys. Rev. A **46**, 5214 (1992).
[12] B. A. Malomed, D. K. Campbell, N. Knowles, and R. Flesch, Phys. Lett. A **178**, 271 (1993).
[13] A. J. Sievers and S. Takeno, Phys. Rev. Lett. **61**, 970 (1988).
[14] S. Takeno, K. Kisoda, and A. J. Sievers, Prog. Theor. Phys. Suppl. **94**, 242 (1988).
[15] A. M. Kosevich and A.S. Kovalev, Zh. Eksp. Teor. Fiz. **67**, 1793 (1974) [Sov. Phys. JETP **40**, 891 (1974)].
[16] B. A. Malomed, J. Phys. A **25**, 755 (1992).
[17] M. Peyrard and A. R. Bishop, Phys. Rev. Lett. **62**, 2755 (1989).
[18] W. H. Press, B. P. Flannery, S. A. Teukolsky, and W. T. Vetterling, *Numerical Recipes* (Cambridge University Press, Cambridge, England, 1989).
[19] O. M. Braun and Yu. S. Kivshar, Phys. Lett. A **149**, 119 (1990).
[20] Yu. S. Kivshar and D. K. Campbell, Phys. Rev. E **48**, 3077 (1993).
[21] O. Bang and M. Peyrard (unpublished).